BIOCHEMISTRY
including biophysical chemistry & molecular biology

Article

pubs.acs.org/biochemistry

Distal Regulation of Heme Binding of Heme Oxygenase-1 Mediated by Conformational Fluctuations

Erisa Harada,[†] Masakazu Sugishima,[‡] Jiro Harada,[‡] Keiichi Fukuyama,[§,∥] and Kenji Sugase*[,†]

[†]Bioorganic Research Institute, Suntory Foundation for Life Sciences, 1-1-1 Wakayamadai, Shimamoto, Mishima, Osaka 618-8503, Japan

[‡]Kurume University School of Medicine, 67 Asahi-machi, Kurume, Fukuoka 830-0011, Japan

[§]Graduate School of Science, Osaka University, Toyonaka, Osaka 560-0043, Japan

Supporting Information

ABSTRACT: Heme oxygenase-1 (HO-1) is an enzyme that catalyzes the oxidative degradation of heme. Since free heme is toxic to cells, rapid degradation of heme is important for maintaining cellular health. There have been useful mechanistic studies of the HO reaction based on crystal structures; however, how HO-1 recognizes heme is not completely understood because the crystal structure of heme-free rat HO-1 lacks electron densities for A-helix that ligates heme. In this study, we characterized conformational dynamics of HO-1 using NMR to elucidate the mechanism by which HO-1 recognizes heme. NMR relaxation experiments showed that the heme-binding site in heme-free HO-1 fluctuates in concert with a surface-exposed loop and transiently forms a partially unfolded structure. Because the fluctuating loop is located over 17 Å distal from the heme-binding site and its conformation is nearly identical among different crystal structures including catalytic intermediate states, the function of the loop has been unexamined. In the course of elucidating its function, we found interesting mutations in this loop that altered activity but caused little change to the conformation. The Phe79Ala mutation in the loop changed the conformational dynamics of the heme-binding site. Furthermore, the heme binding kinetics of the mutant was slower than that of the wild type. Hence, we concluded that the distal loop is involved in the regulation of the conformational change for heme binding through the conformational fluctuations. Similar to other enzymes, HO-1 effectively promotes its function using the identified distal sites, which might be potential targets for protein engineering.

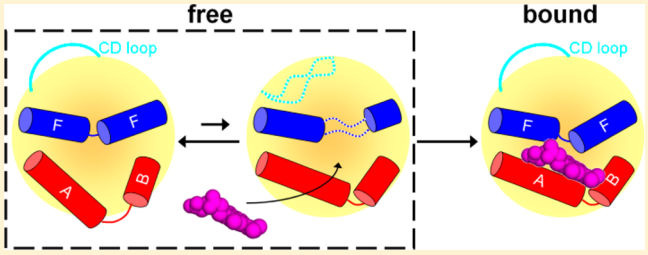

Heme oxygenase-1 (HO-1) is an enzyme that catalyzes the rate-limiting step in the oxidative heme degradation. When electrons are provided by the partner protein cytochrome P450 reductase (CPR), HO-1 cleaves free heme to produce iron, carbon monoxide, and biliverdin-IXα. Since free heme is toxic to cells, HO-1 is important for maintaining cellular health. The degradation products play essential roles in cellular homeostasis.[1−3] Iron from heme strongly contributes to iron homeostasis because heme is the most abundant source of iron[4] and carbon monoxide is a gaseous messenger that exhibits numerous biological functions, such as vascular control and tissue viability.[4] Biliverdin-IXα is immediately reduced to bilirubin-IXα by biliverdin reductase (BVR), and both biliverdin-IXα and bilirubin-IXα are potent scavengers of peroxyl radicals.[1−5] The transcriptional level of HO-1 is regulated by several stress factors, including cytokines, oxidative stresses, and exogenous chemicals, such as heavy metal salts.[4,5] The expression level is associated with a number of diseases, such as diabetes, hypertension, and cancer.[4,5] Therefore, the HO-1 system has been studied as a biomarker and therapeutic target for potential clinical applications.[4,5]

Along with the transcriptional regulation, enzyme catalysis of HO-1 is also regulated by its tertiary structure. In the presence of heme, HO-1 forms a stable complex as though it is behaving a heme enzyme. HO-1 exclusively cleaves the α-meso position of heme, which means that HO-1 specifically recognizes the orientation of heme. Many crystal structures of complexes of the soluble domain, which retains the catalytic activity, have been determined for various states during catalysis, including degraded heme intermediates.[6−11] These studies have shown that the structure is adjusted during the degradation reaction by rearranging the hydrogen-bonding network around the heme-binding site, involving heme and water molecules.[12,13] On the other hand, in the absence of heme, the electron density of the N-terminal region in the crystal structure of rat HO-1 is low and discontinuous.[14] This region includes A-helix, in which His25 axially ligates heme in the heme-bound state. Conformational fluctuations certainly exist in the free state of HO-1, and it is supposed that these fluctuations are important for heme recognition. The mechanism, however, still remains elusive.

Here, we characterized the solution structure and conformational dynamics of HO-1 using NMR to obtain insights into the

Received: August 5, 2014
Revised: December 13, 2014
Published: December 15, 2014

DOI: 10.1021/bi5009694
Biochemistry 2015, 54, 340−348

relationship between the conformational flexibility and heme recognition of the enzyme. As a result, we found that a surface-exposed loop, which is distal to the catalytic center, participates in the regulation of the conformational change of the heme-binding site of heme-free HO-1 through intramolecular fluctuations. This study demonstrates that analyzing conformational fluctuations is important to understand the role of a functional distal site when enzyme activity cannot be explained by static structures alone.

MATERIALS AND METHODS

Sample Preparation. Rat HO-1 (residues 1−232) was expressed and purified as described[15] except for using expression vector pET21a and host cells BL21(DE3). $^{2}H/^{13}C/^{15}N$- and $^{2}H/^{15}N$-labeled HO-1 were prepared by growing cells in minimum M9 medium in 99.9% $^{2}H_2O$ supplemented with ^{15}N ammonium chloride, ^{15}N ammonium sulfate, and ^{12}C (or ^{13}C) glucose as sources of nitrogen and carbon, respectively. The Zn(II) protoporphyrin IX (ZnPP)-bound form of HO-1 was prepared as described under dark conditions.[7] Alanine single point mutants were generated from the wild type using a TOYOBO KOD-Plus mutagenesis kit. Protein concentration was determined spectrophotometrically using a molecular extinction coefficient of 25 900 M^{-1} cm^{-1} at 280 nm for the free state and using the Bradford method for ZnPP-bound state. Recombinant rat CPR, which is solubilized by the truncation of the membrane anchor, was expressed and purified as previously reported.[16] Rat BVR was purified from liver as previously reported.[17]

The chemical shift assignments for the wild-type HO-1 in the free and ZnPP-bound states and F79A HO-1 in the free state were described[18] and deposited in the BioMagResBank under the accession numbers of 18798, 18800, and 18799, respectively.

X-ray Crystallography of ZnPP-Bound HO-1. ZnPP-bound HO-1 was crystallized under similar conditions as those for the heme-bound state.[7] The ZnPP-bound HO-1 crystal mounted on a cryoloop was cooled with liquid nitrogen. Diffraction data were collected at 100 K using synchrotron radiation (λ = 1.2000 Å) at the beamline BL38B1 of SPring-8 (Sayo, Japan, proposal nos. 2010A1179 and 2009B2095) and RIGAKU JUPITER 210 CCD detector. The phases were determined by molecular replacement using the structure of the protein moiety of the heme-bound state (PDB: 1DVE). The obtained model was further refined and manually adjusted with the CCP4 package[19] and Coot.[20] There were seven ZnPP-bound HO-1 molecules in an asymmetric unit, but the appearance of electron density of ZnPP was different in each molecule. Because the electron density of ZnPP in chain A was the clearest, this molecule was used for the comparison with the heme-bound state. Crystallographic data and diffraction statistics are given in Table S1.

Relaxation Dispersion and CLEANEX-PM Experiments. ^{15}N R_2 relaxation dispersion spectra were measured on AVANCE DRX600 and AVANCE DMX750 (Bruker BioSpin) using the TROSY-type constant-time Carr−Purcell−Meiboon−Gill pulse sequence with 40 ms constant relaxation delay.[21] Signal intensities were obtained using the program MUNIN.[22] Relaxation dispersion data were fitted to a two-state exchange model using the program GLOVE.[23,24] The relaxation dispersion curves were initially fitted for each individual residue. Since similar exchange rates were obtained for almost all residues, all relaxation dispersions were fitted with a single set of global parameters of the exchange rate and the minor population. The reduced chi-square value was used to assess the goodness of fit.

CLEANEX-PM spectra were measured with mixing times of 5, 10, 15, 20, 50, and 100 ms at 298 K.[25] Signal intensities were obtained using the program MUNIN,[22] and water and amide proton exchange rates were obtained from the curve fitting of the CLEANEX-PM profiles. The population of the water-exposed state, p_{open}, was calculated according to $p_{open} = k_{ex}/k_{int}$, where k_{ex} represents the water and amide proton exchange rate determined from the CLEANEX-PM experiments[26] and k_{int} represents the intrinsic water and amide proton exchange rate estimated from the amino acid composition using http://www.fccc.edu/research/labs/roder/sphere/.

Modeling A Helix Missing in the Crystal Structure of Heme-Free HO-1. Since the backbone dihedral angles derived from the chemical shifts of A-helix in heme-free HO-1 using the program TALOS+[27] were very similar to those in the crystal structure of heme-bound HO-1, initially, A-helix was constructed using the program MODELLER[28] with the crystal structures of A-helix (residues 11−30) of heme-bound HO-1 and the rest of the protein (residues 31−232) of heme-free HO-1 as templates. Subsequently, energy minimization calculation was performed using the program AMBER.[29,30] During the energy minimization, A-helix was restrained with the dihedral angles obtained from the chemical shifts, and the rest of the protein was fixed.

Heme Degradation and Binding Activities of HO-1. The heme degradation activity of HO-1 was determined as the rate of bilirubin formation in the presence of BVR monitored as the absorbance at 468 nm in 100 mM potassium phosphate buffer (pH 7.4) at 298 K.[31]

The heme-binding rate of HO-1 was determined by real-time UV/vis monitoring of the Soret band after the addition of 460 nM heme to 1 μM HO-1 in 100 mM potassium phosphate buffer (pH 7.0) at 298 K. The real-time UV data ($A_{\text{Soret band}}$) were fitted to the equation

$$A_{\text{Soret band}} = [\text{heme}]\varepsilon_{\text{free}} + [\text{HO-1:heme}]\varepsilon_{\text{bound}} + \text{offset}$$

where $\varepsilon_{\text{free}}$ and $\varepsilon_{\text{bound}}$ represent extinction coefficients of free heme and the HO-1:heme complex, respectively. [heme] and [HO-1:heme] represent the concentrations of free heme and the HO-1:heme complex, respectively, and they are given by

$$[\text{heme}] = \frac{1}{2}\{[\text{heme}]_0 - [\text{HO-1}]_0 - K_D - \Delta\}$$

$$[\text{HO-1:heme}] = \frac{1}{2}\{[\text{heme}]_0 + [\text{HO-1}]_0 + K_D + \Delta\}$$

$$\Delta = \sqrt{\alpha^2 - 4\beta}\,\frac{\exp(-k_{on}\sqrt{\alpha^2 - 4\beta}\,t) + \frac{(\alpha + \sqrt{\alpha^2 - 4\beta})^2}{4\beta}}{\exp(-k_{on}\sqrt{\alpha^2 - 4\beta}\,t) - \frac{(\alpha + \sqrt{\alpha^2 - 4\beta})^2}{4\beta}}$$

$$\alpha = [\text{HO-1}]_0 + [\text{heme}]_0 + K_D$$

$$\beta = [\text{HO-1}]_0[\text{heme}]_0$$

where $[\text{HO-1}]_0$ and $[\text{heme}]_0$ represent the total concentrations of HO-1 and heme, respectively, and K_D is the dissociation constant (k_{off}/k_{on}). The equations are obtained by solving the following simultaneous equations

DOI: 10.1021/bi5009694
Biochemistry 2015, 54, 340−348

$$\begin{cases} [\text{HO-1}] = [\text{HO-1}]_0 - [\text{HO-1:heme}] \\ [\text{heme}] = [\text{heme}]_0 - [\text{HO-1:heme}] \\ \dfrac{d}{dt}[\text{HO-1:heme}] = [\text{HO-1}][\text{heme}]k_{on} \\ \qquad\qquad - [\text{HO-1:heme}]k_{off} \end{cases}$$

RESULTS

Conformational Change of the Heme-Binding Site. We previously determined a number of crystal structures of HO-1 in various states, including the free, heme-bound, verdoheme-bound, and biliverdin-Fe^{3+}-bound states (Figure 1a).[7,8,11,14] Comparisons of these structures indicate that the overall structure is maintained during the catalytic cycle except for the heme-binding site formed by A-, B-, and F-helix. As mentioned above, A-helix is not clearly visible in the crystal structure in the free state. The asymmetric unit of heme-free HO-1 consists of three molecules with different conformations around B- and F-helix. The hydrogen-bonding patterns are slightly different between the three conformations, thus the free state of HO-1 should be flexible. Interestingly, B- and F-helix in the three molecules lie along lines toward the heme-bound conformation (Figure 1b). B-helix moves as a hinge connecting A- and F-helix during the catalytic cycle. The existence of these substates implies that conformational equilibrium exists in the free state, and we assumed that this directional movement is associated with the heme recognition by HO-1. This assumption is supported by a previous normal-mode analysis showing that the flexibility of the heme-binding site of heme-free HO-1 is closely related to the conformational change for heme binding.[32]

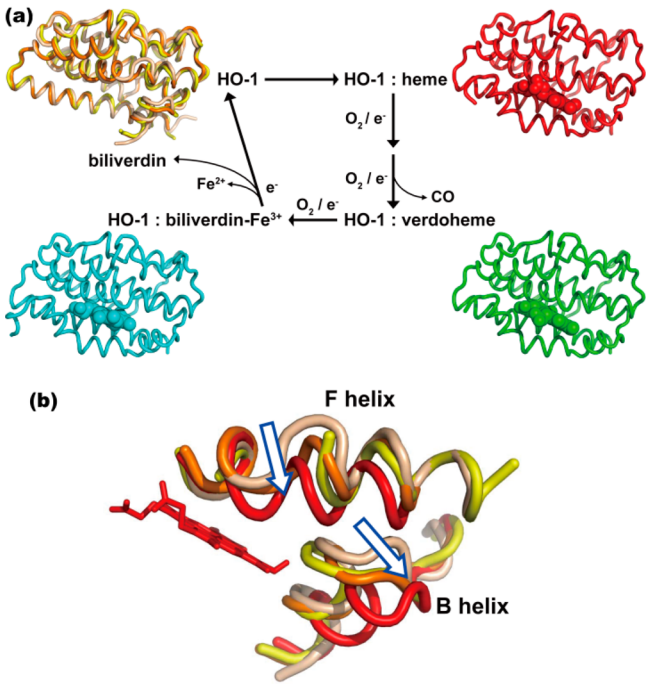

Figure 1. Conformational changes of HO-1 during the catalysis of heme degradation. (a) Crystal structures of HO-1 in the free state (light yellow, yellow, and orange; PDB: 1IRM), the heme-bound state (red; PDB: 1DVE), the verdoheme-bound state (green; PDB: 2ZVU), and the biliverdin-Fe^{3+}-bound state (blue; PDB: 1J2C). Heme, verdoheme, and biliverdin are represented as space-filling models. (b) Closed view of B- and F-helix in superposition of the free and heme-bound states. The arrows indicate putative movements of the free structures toward the heme-bound structure.

To gain further insight into how the heme-binding process of HO-1 is regulated by conformational flexibility, we characterized the solution structure of HO-1 using NMR. Initially, we confirmed that the secondary structures of HO-1 in the free and bound states are consistent with those of the crystal structures by analysis of chemical shifts[27] (Figures S1 and S2). Interestingly, the structure of A-helix of heme-free HO-1 exists, although it is not found in the crystal.[14] Thus, A-helix would fluctuate in solution while maintaining its helical structure, and this fluctuation would have rendered its electron density unobservable. For the bound state, we used Zn(II)-protoporphyrin IX (ZnPP) instead of heme to avoid the paramagnetic relaxation effect. The ZnPP-bound crystal structure was identical to that of heme-bound HO-1 (Figure S3 and Table S1). Chemical shift changes induced by ZnPP binding were primarily localized at A-, B-, and F-helix[18] corresponding to the regions that undergo conformational changes from the free to the heme-bound state in the crystal (Figure S1b).

Conformational Fluctuations of HO-1. Since conformational changes related to enzymatic reactions involving ligand binding typically occur on the millisecond time scale, we conducted ^{15}N relaxation dispersion experiments to examine conformational fluctuations on this time scale in the protein.[19,23,33] In the case of heme-free HO-1, fluctuations of the heme-binding site (A-, B-, and F-helix; Figure 2a) were

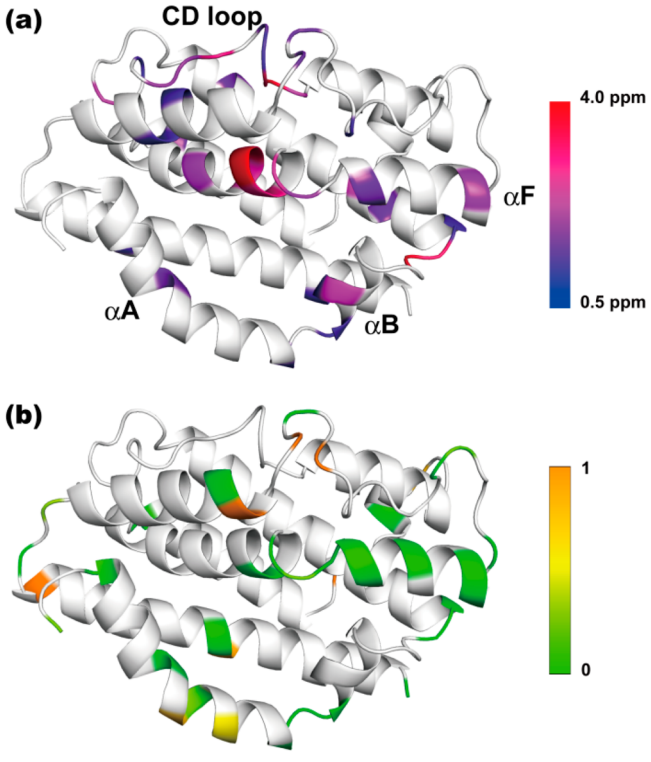

Figure 2. Conformational dynamics of heme-free HO-1. (a) Chemical shift differences, $\Delta\omega$, between the major and minor states. $\Delta\omega$ values are plotted on the structure of heme-free HO-1 as a continuous color scheme from blue to red. (b) The population of the water-exposed open state, p_{open}, calculated from the water and amide proton exchange rates. p_{open} values are plotted on the structure of heme-free HO-1 as a continuous color scheme from green ($p_{open} > 0$) to orange ($p_{open} \approx 1$).

DOI: 10.1021/bi5009694
Biochemistry 2015, 54, 340−348

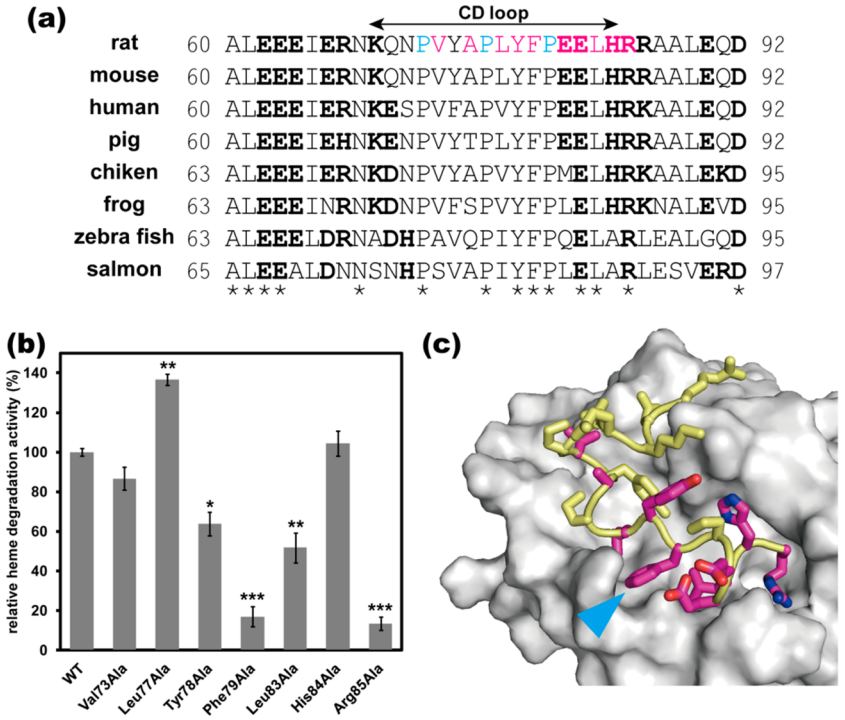

Figure 3. Relationship between the amino acid sequences of CD-loop and conformational fluctuation. (a) Sequence alignments of the residues in the vicinity of CD-loop. The fluctuating residues identified by the relaxation dispersion experiments and proline residues are shown in magenta and blue, respectively. Charged residues (Arg, Lys, His, Asp, and Glu) are highlighted in bold. Asterisks indicate conserved residues among the eight species. (b) Heme degradation activities of HO-1 and alanine point mutants. The mean value and standard deviation of relative heme degradation activities were obtained from triplicate measurements. Mutant activities were evaluated by using a paired *t*-test. $^{*}P < 0.05$, $^{**}P < 0.01$, and $^{***}P < 0.001$. (c) Closed view of the crystal structure in the vicinity of CD-loop. The backbone of CD-loop and the side chains of the fluctuating residues are represented as a tube and sticks, respectively. Other regions are shown as a surface model. Carbon, nitrogen, and oxygen atoms are colored magenta, blue, and red, respectively. The cyan triangle points to the position of Phe79.

observed. Unexpectedly, a surface-exposed loop (CD-loop) also fluctuated, although it is 17 Å distal to the heme-binding site and its conformation remained unchanged during the catalysis both in the crystal and in solution (Figure 1a and Figure S1b). Thus, the function of CD-loop has not been examined previously. All relaxation dispersion profiles were globally fitted well to a two-state exchange model with a rate of the conformational change $k_{\mathrm{minor}\rightarrow\mathrm{major}}$ of 1904 ± 29 s^{-1} and a minor population of 1.7 ± 0.07%, indicating that different regions involving the heme-binding site and the protein surface fluctuate cooperatively. Many hydrophobic residues that form intramolecular interactions with each other were shown to fluctuate and thus they should connect the fluctuations observed in the different regions. Interestingly, all of the fluctuations were suppressed by adding ZnPP. Since CD-loop has no direct contact with ZnPP, this result indicates that the fluctuation in CD-loop is coupled to those in the heme-binding site through intramolecular interactions.

To characterize the fluctuations of heme-free HO-1 in more detail, we attempted to analyze chemical shift differences, $\Delta\omega$, which were determined by the relaxation dispersion experiments. $\Delta\omega$ roughly represents the magnitude of the conformational difference between the major and minor states (Figure 2a). The $\Delta\omega$ values are usually compared to chemical shift differences determined by other experiments. However, comparison of $\Delta\omega$ to the chemical sift differences between the free and ZnPP-bound states was difficult because the chemical shifts in the ZnPP-bound states were changed by the ring current shifts from ZnPP as well as the conformational change from the free states. To complement the structural analysis of the fluctuations of HO-1, we additionally performed CLEANEX-PM experiments,[25] which provide water and amide proton exchange rates of a protein on the millisecond to subsecond time scales. The conformational fluctuations that cause proton exchange should be faster than the proton exchange rates; thus, the time scales of conformational fluctuations analyzed by CLEANEX-PM cover those of fluctuations detected by relaxation dispersion experiments. Interestingly, F-helix, especially around the kink Gly143−Gly144, was shown to adopt a water-exposed open conformation (Figure 2b). This kink is highly conserved and important for HO-1 activity.[34] Since the open population, p_{open}, is less than 1, F-helix would be partially frayed or unfolded during the fluctuation. Similarly, a kink region in A-helix, which is close to the heme ligating His25, also showed CLEANEX-PM peaks, suggesting a fluctuation into a partially unfolded structure. Since the water and amide proton exchange of A- and F-helix was suppressed in the ZnPP-bound state of HO-1 (Figure S4), the final bound conformation of A- and F-helix would be induced by heme binding. On the other hand, no water-exchange signal was observed for CD-loop, which was also shown to fluctuate by the relaxation dispersion experiments (Figure 2b). This result suggests that CD-loop fluctuates in the protein interior composed of many hydrophobic residues while being protected from water. Thus, the fluctuation of CD-loop should be propagated to adjacent regions through the hydrophobic interactions.

DOI: 10.1021/bi5009694
Biochemistry 2015, 54, 340−348

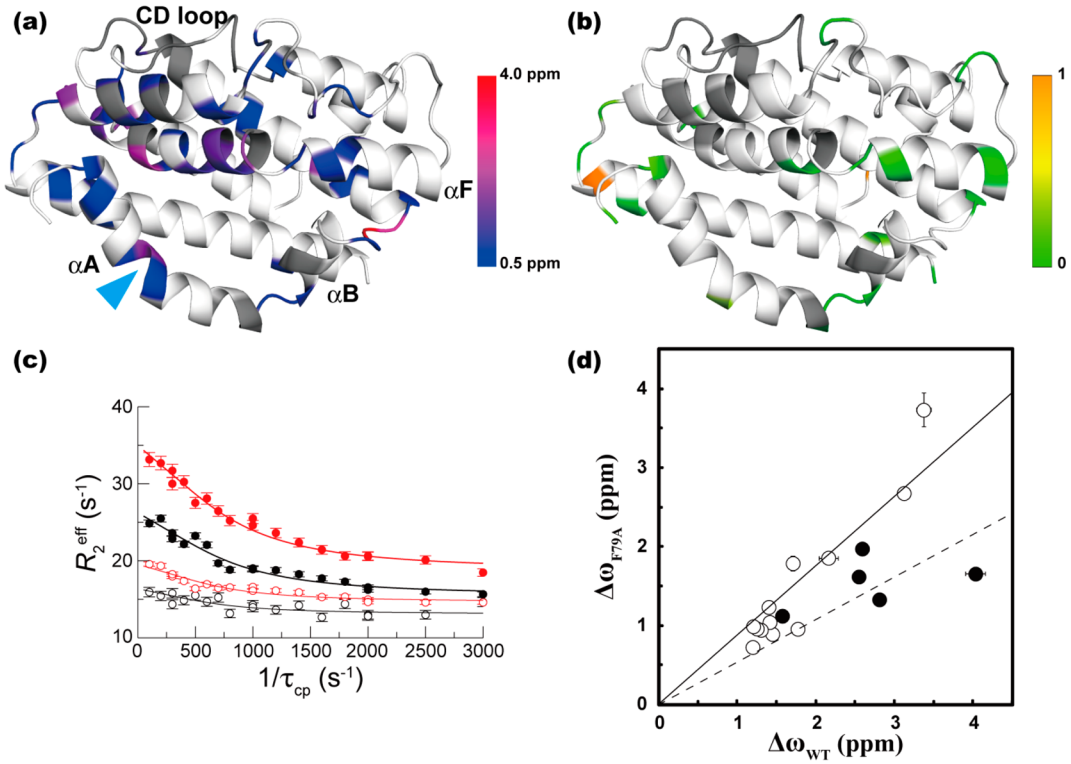

Figure 4. Alteration in conformational dynamics of HO-1 in the free state by the Phe79Ala mutation. (a) Chemical shift differences of F79A HO-1, $\Delta\omega_{F79A}$, plotted on the structure in the same manner as in Figure 2a. The residues whose NMR signals were missing due to line broadening are shown in dark gray. The cyan triangle points to the position of Thr21. (b) The population of the water-exposed open state of F79A HO-1, p_{open}, plotted on the structure in the same manner as in Figure 2b. (c) Relaxation dispersion profiles of Thr21 in the wild-type (open circles) and F79A HO-1 (filled circles) collected at ^{15}N frequencies of 76.0 MHz (red) and 60.8 MHz (black). (d) The correlation of $\Delta\omega$ between the wild-type and F79A HO-1. Filled and open circles represent residues in F-helix and other residues, respectively. The slopes of $\Delta\omega_{F79A}/\Delta\omega_{WT}$ for F-helix and other regions are 0.54 (dotted line) and 0.88 (solid line), respectively. The slopes are significantly different by an F test.

Functional Role of CD-Loop in the Enzymatic Reaction of HO-1. The amino acid sequence of CD-loop is unique in that a cluster of proline and hydrophobic residues is sandwiched by hydrophilic residues. This unique sequence is highly conserved among vertebrates (Figure 3a) compared to that for the other loop regions in HO-1, which implies that CD-loop plays a specific role in HO-1 function. The observation of the cooperative fluctuations among CD-loop and other regions led us to hypothesize that CD-loop remotely regulates the enzyme function through intramolecular interactions. To test this hypothesis, we created a series of alanine single point mutants of the residues that showed relaxation dispersions in CD-loop. As expected, the heme degradation activity was altered by the mutations, and, surprisingly, the activities of F79A and R85A mutants were reduced to less than 20% (Figure 3b). Since Phe79 is located in the middle of CD-loop, we focused on F79A HO-1 in the following analyses (Figure 3c).

First, we confirmed that the F79A mutation does not change the secondary structure and the backbone dihedral angles using circular dichroism and NMR (Figure S5). We also confirmed that the heme-bound structure of this mutant, represented as the Soret absorption in a UV/vis spectrum, was identical to that of the wild type. Furthermore, ^{15}N heteronuclear NOEs were virtually identical between the wild-type and F79A HO-1 in the free state (Figure S6). These data suggests that the static structure of HO-1 and protein motions on picosecond to nanosecond time scales were not affected by the mutation. To address whether the decrease in the heme degradation activity resulted from impaired substrate-binding affinity, we subsequently monitored the heme-binding process in real time using UV/vis (Figure S7). The determined dissociation rates k_{off} were extremely slow (<10^{-3} s^{-1}) for the wild-type and F79A HO-1, indicating that heme rarely dissociated during the experiments. Thus, the association process is the determinant of the heme-binding activity. The determined k_{on} values (4163 ± 1 M^{-1} s^{-1} for the wild type and 2934 ± 77 M^{-1} s^{-1} for the F79A mutant) are on the same order of magnitude as the heme association rates of apo cytochrome b_5 obtained by stopped-flow analyses (1500, 2700 M^{-1} s^{-1}).[35] Since k_{on} of F79A HO-1 was slower than that of the wild type, we concluded that CD-loop remotely regulates the heme association process.

To further understand the structural properties that contribute to the heme association process, we investigated fluctuations of F79A HO-1, as any apparent static conformational change induced by the mutation was not observed (Figures S5 and S6). We found that some NMR signals of the residues around the mutated site Ala79 and those of A- and B-helix were missing due to line broadening (Figure 4a). Furthermore, all observed relaxation dispersion profiles were significantly altered by the mutation, for example, Thr21 in A-helix (Figure 4c). These results indicate that the mutational effect was propagated as far as to the opposite side of the protein. The rate of the conformational change became faster (2183 ± 31 s^{-1}) and the minor population increased to 6.0 ± 0.6% in F79A HO-1 compared to the wild type. It is noteworthy that F79A HO-1 undergoes less conformational change between the major and minor states than the wild type

DOI: 10.1021/bi5009694
Biochemistry 2015, 54, 340−348

because almost all $\Delta\omega$ values of this mutant are smaller than those of the wild type (Figure 4d). An F test showed that $\Delta\omega$ values in F-helix of F79A HO-1 are especially smaller than other regions, indicating that F-helix adopts a less unfolded structure in the minor state. The less unfolded structure is also supported by the CLEANEX-PM experiments, because fewer residues are water-exposed in F79A HO-1 than in the wild type (Figures 2b and 4b). An alanine substitution for Phe79 should change the hydrophobic packing around CD-loop in the minor state, perturbing the minor conformation of F-helix through intramolecular hydrophobic interactions. The transiently formed minor conformation of F79A HO-1 would thus be less suitable for heme binding since its k_{on} was slower.

DISCUSSION

Our data showed that the heme-binding site of HO-1 cooperatively fluctuates with the distal loop (CD-loop) in the absence of heme. We found that CD-loop is involved in the regulation of the conformational fluctuation of the heme-binding site, which transiently forms a partially unfolded structure to facilitate heme binding (Figure 5). Our findings

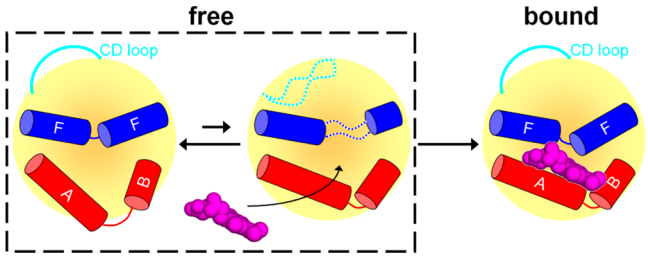

Figure 5. The heme-binding mechanism by the hidden distal effect in HO-1. A- and B-helix are shown as red cylinders, and F-helix, as blue cylinders. CD-loop is represented by cyan lines, and heme is shown by a space-filling model in purple. In heme-free HO-1, A- and B-helix fluctuate for heme binding, and F-helix and CD-loop are partially unfolded in the minor state, as shown by the dotted lines. These two fluctuations are coupled in HO-1. The fluctuation of CD-loop remotely regulates the minor conformation of F-helix that is responsible for heme binding. The final heme-bound structure of the heme-binding site is induced by heme binding.

suggest that the fluctuations in heme-free HO-1 are elaborately organized for heme binding. We also showed that A-helix, which was not visible in the crystal structure, exists in solution. It should be noted that the crystal structure of human HO-1 in the free state has A-helix,[9] whose conformation is similar to the heme-bound structure of human HO-1 (and to the heme-bound structure of rat HO-1). In A-helix and the N-terminal end of B-helix, three amino acids are different between rat and human HO-1: Ile26/Val26, Arg27/Gln27, and Ser31/Ala31 (rat/human). Therefore, these residues might be relevant to the conformational fluctuation in A-helix.

The relaxation dispersion experiments indicated that the fluctuation of CD-loop in free rat HO-1 was suppressed by ZnPP. Li et al. showed that the $^1H/^2H$ exchange rate of Arg85 in CD-loop of human HO-1 was much faster for the free state than for the 2,4-dimethyldeuterohemin (DMDH)-CN^--bound state (0.017 vs 0.00067 s^{-1}),[36] indicating that the contact between helices C and D is flexible in the free state but is stabilized in the DMDH−CN^--bound state.[36] Note that these $^1H/^2H$ exchange rates are beyond the time scale of CLEANEX-PM (0.14−50.82 s^{-1} in Table S3) and thus we did not observe water and amide proton exchange of CD-loop for free or ZnPP-bound rat HO-1 by CLEANEX-PM (Figures 2b and S4). Together with the sequence similarity of CD-loop (Figure 3a), it is suggested that CD-loop in heme-free HO-1 from other organisms is also flexible and takes part in heme recognition. As for the fluctuation in the heme-binding site, local unfolding or coil-to-helix transition around the heme-binding sites has been observed for other hemeproteins such as cytochrome *c*,[37] cytochrome b_5,[38] and heme-regulated transporter regulator.[39] Therefore, it is most likely that the local unfolding around heme-binding sites in hemeproteins is commonly required for the heme-binding process.

In the heme-bound state of HO-1, the orientation of heme is strictly fixed by salt bridges and hydrogen bonds between the propionate groups in heme and the protein and by the orientation of the imidazole plane of heme-ligating His25, enabling HO-1 to cleave heme at the α-meso position selectively.[40] It is conceivable that the orientation of heme before binding is random and that the correct configuration of heme in HO-1 is searched for during the heme-binding process. Interestingly, the kinetic rates $k_{major\rightarrow minor}$ is on the same order of magnitude as the rate of heme in-plane rotation about the iron−His bond (10^2 to 10^3 s^{-1}).[41] Therefore, it is possible that the fluctuation we observed is related to the rotational motion of heme in the heme-binding site.

Recently, the crystal structure of heme-bound HO-1 in complex with an open-conformation-stabilized CPR mutant was determined.[42] The CPR mutant mainly interacts with the surface of F- and G-helix in HO-1 and also contacts with Pro76 in CD-loop. It has been shown that only heme-bound HO-1 associates with wild type[31] or the CPR mutant and that wild-type CPR binds to heme-bound HO-1 with 10-fold weaker affinity than the CPR mutant. Therefore, CPR may not be involved in the distal regulation of the heme-binding process of HO-1 by CD-loop. Since our study showed that the fluctuations observed for heme-free HO-1 were suppressed by heme binding, this suggests that the HO-1 structure stabilized by heme is required for the interaction with CPR and that the fluctuation in CD-loop may be involved in the discrimination between heme-bound and -free states by CPR. On the other hand, the heme degradation catalysis is a multistep reaction involving heme binding, the oxidation of heme, and the release of the products (Figure 1a). Conformational changes of HO-1 during the catalytic cycle are closely related to the enzymatic reaction. For example, a drastic movement of F-helix is important for the discrimination between CO and O_2 molecules.[43,44] Thus, the conformation of the CPR−HO-1 complex may also be rearranged during the catalytic cycle. We speculate that the conformational rearrangement of the CPR−HO-1 complex changes the contact surface between CPR and HO-1, which enables CPR to interact with CD-loop more tightly and influence some catalytic steps through the interaction with CD-loop. In this study, we examined the influence of CD-loop on the heme-binding process. We observed that the F79A mutation decreased the heme-binding rate by 30% compared to the wild type. This reduction is smaller than that of the heme degradation activity (83%), indicating that CD-loop contributes to other heme degradation processes in addition to the heme-binding process. Therefore, the role of CD-loop in the catalytic cycle is still to be elucidated.

There has been growing evidence that functional fluctuations are exquisitely programmed in amino acid sequences together

DOI: 10.1021/bi5009694
Biochemistry 2015, 54, 340−348

with tertiary structures.[45−48] It has been reported that the major conformation and/or the frequency of internal motions can be modified by a mutation or an effector molecule through fluctuations.[49−52] For several enzymes, such as human proline isomerase cyclophilin A and dihydrofolate reductase, conformational equilibrium shifts have been reported.[52,53] In the case of the catabolite activator protein, an allosteric effector, cyclic AMP, shifts the internal motion.[54] By contrast, the current study addresses a new mechanism in which a distal site regulates the minor conformation of the active site via the fluctuations without changing the major conformation of the protein. It is possible that many proteins exploit such distal effects to exert their functions; however, most distal sites have been overlooked due to technical difficulties. Here, we designate this type of molecular regulation as a hidden distal effect. Distal sites have recently drawn attention as potential targets for drug development and protein engineering because a small molecule that binds to a distal site with which a natural ligand does not interact can be utilized as an engineering effector.[55] Our study opens a new avenue for the fundamental understanding of protein functions and practical applications for protein engineering and provides a novel stratagem for drug design.

■ ASSOCIATED CONTENT

Supporting Information

Figure S1: Structural difference between the free and bound states of HO-1. Figure S2: Comparison of HO-1 secondary structures between the crystal and solution states. Figure S3: Comparison of the crystal structures between the heme-bound and ZnPP-bound states. Figure S4: Water-exchangeable residues in the ZnPP-bound state of HO-1. Figure S5: Comparison of backbone dihedral angles between the wild-type and Phe79Ala HO-1 in the free state in solution. Figure S6: ^{15}N heteronuclear NOE deta of the wild-type and Phe79Ala HO-1. Figure S7: Real-time UV/vis monitoring of heme binding to HO-1. Table S1: Data collection and refinement statistics for the ZnPP-bound state. Table S2: Chemical shift differences of the wild-type and Phe79Ala HO-1 in the free state obtained from the relaxation dispersion experiments. Table S3: Water and amide proton exchange rates determined by CLEANEX-PM experiments for the wild-type HO-1 in the heme-free and ZnPP-bound states and Phe79Ala HO-1 in the free state. This material is available free of charge via the Internet at http://pubs.acs.org.

■ AUTHOR INFORMATION

Corresponding Author

*Phone: +81-75-962-7484; Fax: +81-75-962-2115; E-mail: sugase@sunbor.or.jp.

Present Address

‖(K.F.) Graduate School of Engineering, Osaka University, Suita, Osaka 565-0871, Japan.

Author Contributions

E.H. and K.S. designed the experiments; E.H., M.S., and J.H. conducted experiments; and E.H., M.S., J.H., K.F., and K.S. wrote the manuscript.

Funding

This work was supported by Grants-in-Aid for Scientific Research to K.S., M.S., J.H., and K.F. from MEXT and JSPS of Japan.

Notes

The authors declare no competing financial interest.

■ ACKNOWLEDGMENTS

We thank Dr. Naohiro Kobayashi of Osaka University for assistance with NMR chemical shift assignments. We also thank Prof. Masato Noguchi of Teikyo University and Prof. Makoto Suematsu of Keio University for their helpful suggestions.

■ ABBREVIATIONS

HO-1, heme oxygenase-1; CPR, cytochrome P450 reductase; BVR, biliverdin reductase; ZnPP, Zn(II) protoporphyrin IX

■ REFERENCES

(1) Kikuchi, G., Yoshida, T., and Noguchi, M. (2005) Heme oxygenase and heme degradation. *Biochem. Biophys. Res. Commun. 338*, 558−567.

(2) Verma, A., Hirsch, D. J., Glatt, C. E., Ronnett, G. V., and Snyder, S. H. (1993) Carbon monoxide: a putative neural messenger. *Science 259*, 381−384.

(3) Suematsu, M., Goda, N., Sano, T., Kashiwagi, S., Egawa, T., Shinoda, Y., and Ishimura, Y. (1995) Carbon monoxide: an endogenous modulator of sinusoidal tone in the perfused rat liver. *J. Clin. Invest. 96*, 2431−2437.

(4) Abraham, N., and Kappas, A. (2008) Pharmacological and clinical aspects of heme oxygenase. *Pharmacol. Rev. 60*, 79−127.

(5) Ryter, S., Alam, J., and Choi, A. (2006) Heme oxygenase-1/carbon monoxide: from basic science to therapeutic applications. *Physiol. Rev. 86*, 583−650.

(6) Schuller, D. J., Wilks, A., Ortiz de Montellano, P. R., and Poulos, T. L. (1999) Crystal structure of human heme oxygenase-1. *Nat. Struct. Biol. 6*, 860−867.

(7) Sugishima, M., Omata, Y., Kakuta, Y., Sakamoto, H., Noguchi, M., and Fukuyama, K. (2000) Crystal structure of rat heme oxygenase-1 in complex with heme. *FEBS Lett. 471*, 61−66.

(8) Sugishima, M., Sakamoto, H., Higashimoto, Y., Noguchi, M., and Fukuyama, K. (2003) Crystal structure of rat heme oxygenase-1 in complex with biliverdin-iron chelate. Conformational change of the distal helix during the heme cleavage reaction. *J. Biol. Chem. 278*, 32352−32358.

(9) Lad, L., Schuller, D. J., Shimizu, H., Friedman, J., Li, H., Ortiz de Montellano, P. R., and Poulos, T. L. (2003) Comparison of the heme-free and -bound crystal structures of human heme oxygenase-1. *J. Biol. Chem. 278*, 7834−7843.

(10) Lad, L., Friedman, J., Li, H., Bhaskar, B., Ortiz de Montellano, P. R., and Poulos, T. L. (2004) Crystal structure of human heme oxygenase-1 in a complex with biliverdin. *Biochemistry 43*, 3793−3801.

(11) Sato, H., Sugishima, M., Sakamoto, H., Higashimoto, Y., Shimokawa, C., Fukuyama, K., Palmer, G., and Noguchi, M. (2009) Crystal structure of rat haem oxygenase-1 in complex with ferrous verdohaem: presence of a hydrogen-bond network on the distal side. *Biochem. J. 419*, 339−345.

(12) Syvitski, R. T., Li, Y., Auclair, K., Ortiz De Montellano, P. R., and La Mar, G. N. (2002) ^{1}H NMR detection of immobilized water molecules within a strong distal hydrogen-bonding network of substrate-bound human heme oxygenase-1. *J. Am. Chem. Soc. 124*, 14296−14297.

(13) Rodríguez, J. C., Zeng, Y., Wilks, A., and Rivera, M. (2007) The hydrogen-bonding network in heme oxygenase also functions as a modulator of enzyme dynamics: chaotic motions upon disrupting the H-bond network in heme oxygenase from *Pseudomonas aeruginosa*. *J. Am. Chem. Soc. 129*, 11730−11742.

(14) Sugishima, M., Sakamoto, H., Kakuta, Y., Omata, Y., Hayashi, S., Noguchi, M., and Fukuyama, K. (2002) Crystal structure of rat apo-heme oxygenase-1 (HO-1): mechanism of heme binding in HO-1 inferred from structural comparison of the apo and heme complex forms. *Biochemistry 41*, 7293−7300.

DOI: 10.1021/bi5009694
Biochemistry 2015, 54, 340−348

(15) Omata, Y., Asada, S., Sakamoto, H., Fukuyama, K., and Noguchi, M. (1998) Crystallization and preliminary X-ray diffraction studies on the water soluble form of rat heme oxygenase-1 in complex with heme. *Acta Crystallogr., Sect. D: Biol. Crystallogr. 54*, 1017−1019.
(16) Hayashi, S., Omata, Y., Sakamoto, H., Hara, T., and Noguchi, M. (2003) Purification and characterization of a soluble form of rat liver NADPH-cytochrome P-450 reductase highly expressed in *Escherichia coli*. *Protein Expression Purif. 29*, 1−7.
(17) Yoshida, T., and Kikuchi, G. (1979) Purification and properties of heme oxygenase from rat liver microsomes. *J. Biol. Chem. 254*, 4487−4491.
(18) Harada, E., Sugishima, M., Harada, J., Noguchi, M., Fukuyama, K., and Sugase, K. (2014) Backbone assignments of the apo and Zn(II) protoporphyrin IX-bound states of the soluble form of rat heme oxygenase-1. *Biomol. NMR Assignments*, DOI: 10.1007/s12104-014-9573-z.
(19) Collaborative Computational Project No. 4 (1994) The CCP4 suite: programs for protein crystallography. *Acta Crystallogr., Sect. D: Biol. Crystallogr. 50*, 760−763.
(20) Emsley, P., Lohkamp, B., Scott, W. G., and Cowtan, K. (2010) Features and development of Coot. *Acta Crystallogr., Sect. D: Biol. Crystallogr. 66*, 486−501.
(21) Loria, J. P., Rance, M., and Palmer, A. G. (1999) A relaxation-compensated Carr−Purcell−Meiboom−Gill sequence for characterizing chemical exchange by NMR spectroscopy. *J. Am. Chem. Soc. 121*, 2331−2332.
(22) Korzhneva, D. M., Ibraghimov, I. V., Billeter, M., and Orekhov, V. Y. (2001) MUNIN: application of three-way decomposition to the analysis of heteronuclear NMR relaxation data. *J. Biomol. NMR 21*, 263−268.
(23) Sugase, K., Lansing, J. C., Dyson, H. J., and Wright, P. E. (2007) Tailoring relaxation dispersion experiments for fast-associating protein complexes. *J. Am. Chem. Soc. 129*, 13406−13407.
(24) Sugase, K., Konuma, T., Lansing, J. C., and Wright, P. E. (2013) Fast and accurate fitting of relaxation dispersion data using the flexible software package GLOVE. *J. Biomol. NMR 56*, 275−283.
(25) Hwang, T. L., Van Zijl, P. C., and Mori, S. (1998) Accurate quantitation of water-amide proton exchange rates using the phase-modulated CLEAN chemical EXchange (CLEANEX-PM) approach with a Fast-HSQC (FHSQC) detection scheme. *J. Biomol. NMR 11*, 221−226.
(26) Krishna, M. M. G., Hoang, L., Lin, Y., and Englander, S. W. (2004) Hydrogen exchange methods to study protein folding. *Methods 34*, 51−64.
(27) Shen, Y., Delaglio, F., Cornilescu, G., and Bax, A. (2009) TALOS+: a hybrid method for predicting protein backbone torsion angles from NMR chemical shifts. *J. Biomol. NMR 44*, 213−223.
(28) Martí-Renom, M. A., Stuart, A. C., Fiser, A., Sánchez, R., Melo, F., and Sali, A. (2000) Comparative protein structure modeling of genes and genomes. *Annu. Rev. Biophys. Biomol. Struct. 29*, 291−325.
(29) Pearlman, D. A., Case, D. A., Caldwell, J. W., Ross, W. S., Cheatham, T. E., Debolt, S., Ferguson, D., Seibel, G., and Kollman, P. (1995) Amber, a package of computer-programs for applying molecular mechanics, normal-mode analysis, molecular-dynamics and free-energy calculations to simulate the structural and energetic properties of molecules. *Comput. Phys. Commun. 91*, 1−41.
(30) Case, D. A., Cheatham, T. E., Darden, T., Gohlke, H., Luo, R., Merz, K. M., Onufriev, A., Simmerling, C., Wang, B., and Woods, R. J. (2005) The Amber biomolecular simulation programs. *J. Comput. Chem. 26*, 1668−1688.
(31) Higashimoto, Y., Sakamoto, H., Hayashi, S., Sugishima, M., Fukuyama, K., Palmer, G., and Noguchi, M. (2005) Involvement of NADPH in the interaction between heme oxygenase-1 and cytochrome P450 reductase. *J. Biol. Chem. 280*, 729−737.
(32) Maréchal, J.-D., and Perahia, D. (2008) Use of normal modes for structural modeling of proteins: the case study of rat heme oxygenase 1. *Eur. Biophys. J. 37*, 1157−1165.
(33) Sugase, K., Dyson, H. J., and Wright, P. E. (2007) Mechanism of coupled folding and binding of an intrinsically disordered protein. *Nature 447*, 1021−1025.
(34) Liu, Y., Lightning, L. K., Huang, H., Moënne-Loccoz, P., Schuller, D. J., Poulos, T. L., Loehr, T. M., and Ortiz de Montellano, P. R. (2000) Replacement of the distal glycine 139 transforms human heme oxygenase-1 into a peroxidase. *J. Biol. Chem. 275*, 34501−34507.
(35) Ihara, M., Takahashi, S., Ishimori, K., and Morishima, I. (2000) Functions of fluctuation in the heme-binding loops of cytochrome b_5 revealed in the process of heme incorporation. *Biochemistry 39*, 5961−5970.
(36) Li, Y., Syvitski, R. T., Auclair, K., de Montellano, P. R. O., and La Mar, G. N. (2004) ^{1}H NMR investigation of the solution structure of substrate-free human heme oxygenase: comparison to the cyanide-inhibited, substrate-bound complex. *J. Biol. Chem. 279*, 10195−10205.
(37) Sagle, L. B., Zimmermann, J., Matsuda, S., Dawson, P. E., and Romesberg, F. E. (2006) Redox-coupled dynamics and folding in cytochrome *c*. *J. Am. Chem. Soc. 128*, 7909−7915.
(38) Mukhopadhyay, K., and Lecomte, J. T. J. (2004) A relationship between heme binding and protein stability in cytochrome b_5. *Biochemistry 43*, 12227−12236.
(39) Sawai, H., Yamanaka, M., Sugimoto, H., Shiro, Y., and Aono, S. (2012) Structural basis for the transcriptional regulation of heme homeostasis in *Lactococcus lactis*. *J. Biol. Chem. 287*, 30755−30768.
(40) Ogura, H., Evans, J., Ortiz de Montellano, P. R., and La Mar, G. N. (2008) Implication for using heme methyl hyperfine shifts as indicators of heme seating as related to stereoselectivity in the catabolism of heme by heme oxygenase: in-plane heme. *Biochemistry 47*, 421−430.
(41) La Mar, G. N., Hauksson, J. B., Dugad, L. B., Liddell, P. A., Venkataramana, N., and Smith, K. M. (1991) Protein NMR study of the heme rotational mobility in myoglobin: the role of propionate salt bridges in anchoring the heme. *J. Am. Chem. Soc. 113*, 1544−1550.
(42) Sugishima, M., Sato, H., Higashimoto, Y., Harada, J., Wada, K., Fukuyama, K., and Noguchi, M. (2014) Structural basis for the electron transfer from an open form of NADPH-cytochrome P450 oxidoreductase to heme oxygenase. *Proc. Natl. Acad. Sci. U.S.A. 111*, 2524−2529.
(43) Sugishima, M., Sakamoto, H., Noguchi, M., and Fukuyama, K. (2003) Crystal structures of ferrous and CO-, CN^--, and NO-bound forms of rat heme oxygenase-1 (HO-1) in complex with heme: structural implications for discrimination between CO and O_2 in HO-1. *Biochemistry 42*, 9898−9905.
(44) Sugishima, M., Moffat, K., and Noguchi, M. (2012) Discrimination between CO and O_2 in heme oxygenase: comparison of static structures and dynamic conformation changes following CO photolysis. *Biochemistry 51*, 8554−8562.
(45) Smock, R. G., and Gierasch, L. M. (2009) Sending signals dynamically. *Science 324*, 198−203.
(46) Henzler-Wildman, K., and Kern, D. (2007) Dynamic personalities of proteins. *Nature 450*, 964−972.
(47) Dunker, A. K., Cortese, M. S., Romero, P., Iakoucheva, L. M., and Uversky, V. N. (2005) Flexible nets. The roles of intrinsic disorder in protein interaction networks. *FEBS J. 272*, 5129−5148.
(48) Tokuriki, N., and Tawfik, D. (2009) Protein dynamism and evolvability. *Science 324*, 203−207.
(49) Goodey, N. M., and Benkovic, S. J. (2008) Allosteric regulation and catalysis emerge via a common route. *Nat. Chem. Biol. 4*, 474−482.
(50) Bahar, I., Chennubhotla, C., and Tobi, D. (2007) Intrinsic dynamics of enzymes in the unbound state and relation to allosteric regulation. *Curr. Opin. Struct. Biol. 17*, 633−640.
(51) Tzeng, S. R., and Kalodimos, C. G. (2011) Protein dynamics and allostery: an NMR view. *Curr. Opin. Struct. Biol. 21*, 62−67.
(52) Boehr, D., Nussinov, R., and Wright, P. E. (2009) The role of dynamic conformational ensembles in biomolecular recognition. *Nat. Chem. Biol. 5*, 789−796.
(53) Fraser, J. S., Clarkson, M. W., Degnan, S. C., Erion, R., Kern, D., and Alber, T. (2009) Hidden alternative structures of proline isomerase essential for catalysis. *Nature 462*, 669−673.

DOI: 10.1021/bi5009694
Biochemistry 2015, 54, 340−348

(54) Tzeng, S. R., and Kalodimos, C. G. (2009) Dynamic activation of an allosteric regulatory protein. *Nature 462*, 368−372.
(55) Hardy, J. A., and Wells, J. A. (2004) Searching for new allosteric sites in enzymes. *Curr. Opin. Struct. Biol. 14*, 706−715.

DOI: 10.1021/bi5009694
Biochemistry 2015, 54, 340−348